



HAL
open science

Chemical labelling of oyster shells used for time-calibrated high-resolution Mg/ca ratios: A tool for estimation of past seasonal temperature variations

Vincent Mouchi, Marc de Rafélis, Franck Lartaud, Michel Fialin, Eric P. Verrecchia

► To cite this version:

Vincent Mouchi, Marc de Rafélis, Franck Lartaud, Michel Fialin, Eric P. Verrecchia. Chemical labelling of oyster shells used for time-calibrated high-resolution Mg/ca ratios: A tool for estimation of past seasonal temperature variations. *Palaeogeography, Palaeoclimatology, Palaeoecology*, 2013, 373 (Special Issue: SI), pp.66-74. 10.1016/j.palaeo.2012.05.023 . hal-00823563

HAL Id: hal-00823563

<https://hal.science/hal-00823563>

Submitted on 27 May 2013

HAL is a multi-disciplinary open access archive for the deposit and dissemination of scientific research documents, whether they are published or not. The documents may come from teaching and research institutions in France or abroad, or from public or private research centers.

L'archive ouverte pluridisciplinaire **HAL**, est destinée au dépôt et à la diffusion de documents scientifiques de niveau recherche, publiés ou non, émanant des établissements d'enseignement et de recherche français ou étrangers, des laboratoires publics ou privés.

1 **Chemical labelling of oyster shells used for time-calibrated high-resolution Mg/Ca**
2 **ratios: a tool for estimation of past seasonal temperature variations**

3 Mouchi Vincent^a, Marc de Rafélis^{a*}, Franck Lartaud^b, Michel Fialin^c, Eric Verrecchia^d

4
5 ^a UPMC Univ Paris 06. UMR 7193 IStEP. Laboratoire Biominéralisations et Environnements
6 Sédimentaires. Case postale 116, 4 place Jussieu, 75005 Paris, France.

7 ^b UPMC Univ Paris 06, CNRS FRE 3350, Laboratoire d'Ecogéochimie des Environnements
8 Benthiques (LECOB), Observatoire Océanologique, av. du Fontaulé, 66650 Banyuls-sur-Mer,
9 France.

10 ^c UPMC Univ Paris 06, Centre Camparis, 4, place Jussieu, 75005 Paris, France.

11 ^d Institut de Géologie et Paléontologie, Université de Lausanne, Anthropole, CH-1015
12 Lausanne, Switzerland.

13
14 * Corresponding author: Marc de Rafelis - ISTEP UMR 7193 UPMC-CNRS - 4 place Jussieu
15 - case courrier 116 - 75005 Paris - France. E-mail: marc.de_rafelis@upmc.fr. Telephone/Fax:
16 +33144274784

17
18 **Abstract:**

19 The geochemical compositions of biogenic carbonates is increasingly used for
20 paleoenvironmental reconstructions. The skeletal $\delta^{18}\text{O}$ temperature relationship is dependent
21 on water salinity, so many recent studies have focused on the Mg/Ca and Sr/Ca ratios because
22 those ratios in water do not change significantly on short time scales. Thus, those elemental
23 ratios are considered to be good paleotemperature proxies in many biominerals, although their
24 use remains ambiguous in bivalve shells. Here, we present the high-resolution Mg/Ca ratios
25 of two modern species of juvenile and adult oyster shells, *Crassostrea gigas* and *Ostrea*

26 *edulis*. These specimens were grown in controlled conditions for over one year in two
27 different locations. *In situ* monthly Mn-marking of the shells has been used for day
28 calibration. The daily Mg/Ca ratios in the shell have been measured with an electron
29 microprobe. The high frequency Mg/Ca variation of all specimens displays good synchronism
30 with lunar cycles, suggesting that tides strongly influence the incorporation of Mg/Ca into the
31 shells. Highly significant correlation coefficients ($0.70 < r < 0.83$, $p < 0.0001$) between the
32 Mg/Ca ratios and the seawater temperature are obtained only for juvenile *C. gigas* samples,
33 while metabolic control of Mg/Ca incorporation and lower shell growth rates preclude the use
34 of the Mg/Ca ratio in adult shells as a paleothermometer. Data from three juvenile *C. gigas*
35 shells from the two study sites are selected to establish a relationship : $T = 3.77Mg/Ca + 1.88$,
36 where T is in °C and Mg/Ca in mmol/mol.

37

38 **Key words:** bivalve shells, seawater temperature, trace elements, growth rates, Mn-markings,
39 cathodoluminescence.

40

41 **1. Introduction**

42 In paleoclimate research, sclerochronology allows the production of high-resolution
43 environmental reconstructions. This type of study is based on the chemical analysis of bivalve
44 mollusc shells, as these organisms build their mineralised carbonate parts from ions that they
45 sample from their environment. Bivalves mineralise their shells by accretion, preventing the
46 destruction of previously secreted parts of the shell. Therefore, this type of material allows the
47 evaluation of water chemistry evolution and environmental variation throughout the life of the
48 organism. Benthic inhabitants from coastal areas are particularly pertinent archives of the
49 paleoclimatic conditions (i.e., seasonal range) because they are affected by temperatures close
50 to those of the surface seawater.

51 The $\delta^{18}\text{O}$ in biogenic carbonates is widely used as a paleothermometer (Klein et al., 1996;
52 Kirby et al., 1998; Andreasson and Schmitz, 2000). Unfortunately, it also depends on
53 seawater isotopic composition (or salinity; Epstein and Mayeda, 1953), which is subject to
54 frequent change. Consequently, this proxy is not always properly constrained (Rohling,
55 2000), particularly in coastal areas where freshwater runoff and/or evaporation occur, and
56 several investigations have been made to estimate salinity, including stable isotopes (Gillikin
57 et al., 2005) and trace elements (Dodd and Crisp, 1982).

58 To obtain more reliable paleotemperatures, other proxies were developed, such as trace
59 elements ratios (Cronblad and Malmgren, 1981; Immenhauser et al., 2005). The Mg/Ca ratio
60 in bivalve shells has been the subject of particularly intensive investigation (Dodd, 1965;
61 Vander Putten et al., 2000; Freitas et al., 2005), but its utility as a reliable seawater
62 thermometer is still unclear, producing positive or negative correlations according to seasonal
63 environmental changes (Freitas et al., 2006). Despite the numerous pertinent studies that
64 present geochemical analyses of recent mollusc shells to quantify the Mg/Ca and Sr/Ca molar
65 ratios as environmental proxies (Boyden and Phillips, 1981; Lazareth et al., 2003; Takesue
66 and van Geen, 2004; Wisshak et al., 2009), few of these works contain both a precise
67 monitoring of the environmental parameters and a sclerochronological calendar of shell
68 growth, both of which are essential to the establishment of a reliable model.

69 Chemical markings in bivalve shells, including fluorochromes and manganese, were
70 developed for shell growth rate and growth pattern estimations (Hawkes et al., 1996; Kaehler
71 and McQuaig, 1999; Lartaud et al., 2010a; Mahe et al., 2010). Several authors showed that
72 manganese markings are particularly effective in the oyster hinge area (Langlet et al., 2006;
73 Barbin et al., 2008), and they can be used to define high-resolution drilling samples of shell
74 carbonate for geochemical analysis (Lartaud et al., 2010b). In this study, we use *Crassostrea*
75 *gigas* and *Ostrea edulis* oyster shells cultured *in situ* coupled with monthly Mn-markings and

76 daily *in situ* hydrological data (i.e., temperature, salinity), which allows a good comparison
77 between the proxy and the environmental conditions. Oyster shells are appropriate for the
78 establishment of a relevant model for seasonal paleo-contrast reconstructions, especially using
79 geochemical investigations. Indeed, oyster shells are primarily composed of low-magnesium
80 calcite, which is the most stable calcium carbonate with respect to diagenesis alteration.
81 Furthermore, oysters are euryhaline molluscs and present large stratigraphic (slow evolution
82 from 200 Ma; Stenzel, 1971), geographic (from intertidal to deep waters), and latitudinal
83 distributions.
84 The purpose of this paper is to investigate the potential of oysters to serve as high-resolution
85 (seasonal) recorders of environmental variations. Using recent specimens from a breeding
86 experiment of two oyster species, *Crassostrea gigas* and *Ostrea edulis*, the evolution of Mg
87 incorporation is measured along the hinge. Geochemical markings, revealed by
88 cathodoluminescence, allow time calibration throughout the growth direction, permitting an
89 effective comparison between the analysed Mg/Ca ratios and the monitored environmental
90 parameters.

91

92 **2. Experimental details**

93 *2.1. Site description*

94 The experiments were carried out in two IFREMER (Institut Français de Recherche pour
95 l'Exploitation de la Mer) marine stations on the French west coast: Baie des Veys
96 (Normandy) and Marennes-Oléron Bay (Charente-Maritime), which are among the largest
97 oyster-farming areas in France (Fig. 1). During the experiment (from February 2005 to
98 November 2006), the environmental parameters such as seawater temperature and salinity
99 were monitored daily using a multi-parameter probe (YSI IFREMER) attached to the
100 breeding tables right next to the packs. According to the measured seawater temperatures, the

101 breeding calendar was split into two main periods, from June to November for the summer
102 period and from December to May for the winter period. Seawater samples for ICP-AES
103 Mg/Ca analysis were collected during the experiment (10 samples at Baie des Veys and 6 at
104 Marennes-Oléron).

105

106 Figure 1

107

108 2.2. *Specimens and rearing strategy*

109 Two different oyster species were selected: the cupped oyster, *Crassostrea gigas* (Thunberg,
110 1793), and the flat oyster, *Ostrea edulis* (Linné, 1758), both of which are mainly calcitic-
111 mineralising molluscs that live in various environments close to the shore (mangrove,
112 estuarine, lagoon, intertidal and subtidal habitats).

113 The details of the breeding conditions for the specimens used in this work are described in
114 Lartaud et al. (2010b) (summarised here in Table 1). Juvenile *C. gigas* were sourced from
115 wild broodstock collected at the Arcachon basin at the end of January 2005. Their date of
116 birth was estimated based on the size of the individuals (< 10 mm from the umbo to the
117 ventral margin) to have been during summer 2004. The spats were separated into several
118 groups and transported in packs to be cultured on oyster tables at the different study locations
119 from the beginning of February 2005 until November 2006 (Table 1). All of these individuals
120 are considered to be juvenile oysters ('jn-gig' prefix on sample code) in contrast to those
121 older than two years, which are considered to be adult specimens in this work.

122 Adult *C. gigas* ('ad-gig' prefix on sample code) were used to study the ontogenic influence on
123 shell Mg/Ca records. These individuals were produced from the IFREMER hatchery at La
124 Tremblade (Charente-Maritime) and transplanted into nursery tanks at Bouin when they
125 remained until they were six months old. The spats were cultured for one year and a half on

126 oyster tables at Marennes-Oléron and then placed in Marennes marine ponds until they joined
127 the marking protocol experiment at the Marennes-Oléron bay site, in September 2005.
128 Adult *O. edulis* ('ad-edu' prefix) were also used to establish the inter-specific calibration of
129 the Mg/Ca proxy based on the analysis of individuals bred under the same environmental
130 conditions. These oysters were born in the summer of 2003 and placed on oyster tables in
131 February 2004 at La Trinité (southern Brittany). At the end of February 2006, they were
132 separated into two groups and transferred to the two study locations.
133 On November 2006, all individuals were sacrificed for shell elemental analysis. In total, four
134 juvenile *C. gigas* shells (one from Marennes-Oléron and three from Baie des Veys), two adult
135 *C. gigas* shells (from Marennes-Oléron) and five adult *O. edulis* shells (three from Baie des
136 Veys, two from Marennes-Oléron) were randomly selected for the high-resolution Mg/Ca
137 ratio analyses.

138

139 Table 1

140

141 To compare the high-resolution geochemical data from the shells and the environmental
142 parameters, a continuous and accurate age model of oyster shells is needed. All individuals
143 were marked on site monthly by placing them in a tank filled with seawater doped with
144 manganese (90 mg/l $MnCl_2$ for 4 hours). The artificial manganese incorporated into the shell
145 calcite is revealed by a highly luminescent micro-growth band under cathodoluminescence
146 (CL) microscopy (Langlet et al., 2006; Barbin et al., 2008). The identification of Mn
147 markings in the shell sections under CL observation allows the precise estimation of growth
148 rates at different time intervals (Lartaud et al., 2010b).

149 The oysters were opened and emptied of their soft tissues immediately after collection. The
150 shells were then placed in a 6% solution of hydrogen peroxide (H_2O_2) for 6 h, washed with a

151 diluted nitric acid (0.15 N for 20 min) and rinsed thoroughly with demineralised water. For
152 each left valve, a 300 μm -thick section was made along the maximum growth axis, through
153 the middle of the hinge region to the ventral shell margin. The microscopic CL and
154 geochemical analyses were performed on the foliated low-magnesium calcite of the hinge
155 section because this area contains a good and well-preserved record of the life of the
156 individual in its environment (Richardson et al., 1993; Kirby et al., 1998; Lartaud et al., 2006;
157 2010c).

158

159 *2.3. Geochemical analysis and data processing*

160 High-resolution analyses of the thin oyster shell sections were carried out with a CAMECA
161 SX 50 electron microprobe (EPMA) at the CAMPARIS service of IStEP, UPMC, Paris. The
162 cations analysed were Mg, Ca and Mn. The operating conditions employed a 25 kV potential
163 with a 130 nA current and a 25 μm defocused beam diameter. The detection limits were 5
164 ppm for Ca, 160 ppm for Mg, and 10 ppm for Mn over a counting-time of 30 seconds. The
165 instrument was calibrated with the following internal standards: a $\text{MgCaSi}_2\text{O}_6$ (diopside)
166 crystal for calcium and magnesium detection and a MnTiO_3 crystal for Mn detection. The
167 totals for analysis ranged between 92 and 100.6 wt% (average total of 96.5 wt%), which are
168 within the acceptable error limits for low-magnesium calcite (England et al., 2007). For each
169 shell, a 1 cm-long transect was chosen parallel to the growth axis, starting from the day of
170 collection and providing 400 measurements per shell. To ensure that the analyses were always
171 performed in a line perpendicular to the micro-increments, the precise location of the transect
172 was made under CL observation prior to EPMA. As defined by Kirby et al. (1998) and
173 Lartaud et al. (2010c), the best sampling zone is located just beneath the ligamental surface
174 area, where the growth increments are all perpendicular to the external edge. The equally
175 spaced analyses were then placed into a calendar scale using both the CL and Mn

176 concentrations (Fig. 2). Because the Mn concentration in oyster shells is naturally very low (at
177 the approximate detection limit of the electron microprobe), the only recognisable spots on
178 the Mn evolution curves of the shells are those that correspond to the Mn-markings. Thus, the
179 geochemical Mn peaks were easily matched to the CL image. Using the AnalySeries software
180 (Paillard et al., 1996) and making the assumption that the shell growth is constant between
181 two consecutive markings, the spatial distribution of the geochemical data was transposed
182 into a time scale with an accuracy that depended on the growth rate of each individual.

183 Once the geochemical data were time calibrated, signal analysis (FFT) was performed to
184 identify the different cyclicities and their meanings. The series were detrended according to
185 the methodology described by Boulila et al. (2008) to remove the low-frequency components
186 of the Mg/Ca curves. Then, the residuals were processed by the Multi-Tapper Method (MTM,
187 Thomson, 1982) using the AnalySeries freeware (Paillard et al., 1996). This method is
188 conventionally used for the analysis of high-noise signals; consequently, it is adapted for
189 natural and metabolic records. To study the seasonal temperature variations, which are
190 considered to be the low frequency signals in this study, the shell Mg/Ca curves were
191 smoothed using a 4-point moving average. The covariations of the shell Mg/Ca ratios with the
192 seawater temperature were studied on the smoothed curves (100 points). For each sample, the
193 overall Mg/Ca temperature relationship was tested with the *Curve Fitting* tool from Matlab (v.
194 7.5.0.342). To ensure the normal distribution of the Mg/Ca-temperature couple residuals, a
195 Kolmogorov-Smirnov test was applied.

196

197 Figure 2

198

199 **3. Results**

200 *3.1. Seawater parameters*

201 At both sites, the environmental records showed small changes in the salinity, with mean
202 values of 33.4 ± 0.7 psu at Baie des Veys and 34.4 ± 2.8 psu at Marennes-Oléron (Table 2,
203 Fig. 3). The episodes of low salinity (down to 28 psu) were recorded in the two stations, but
204 they were clearly linked to rainfall lasting for one or two days. The change in salinity was
205 higher at Marennes-Oléron because of the higher frequency of heavy rain periods. No
206 seasonal variation of the salinity was observed at any site. Conversely, the seawater
207 temperature variations at both sites were related to strong seasonal fluctuations without any
208 relevant correlations with salinity (Figure 3). Throughout the breeding period, the Baie des
209 Veys seawater temperatures ranged from 4.8 to 20.0°C (mean: $12.9 \pm 4.7^\circ\text{C}$), and from 4.8 to
210 23.1°C (mean: $15.0 \pm 5.2^\circ\text{C}$) at Marennes-Oléron. The temperature records are typically
211 sinusoidal, with lower values in the winter and higher values in the summer. The average
212 seawater Mg/Ca ratios are 2.57 ± 0.15 mmol/mol at Baie des Veys (n=10) and 3.25 ± 0.06
213 mmol/mol at Marennes-Oléron (n=6). At both sites, no relationship was observed between the
214 salinity or the temperature and the Mg/Ca ratios of the seawater throughout the year (Table 2).

215

216 Table 2, Figure 3

217

218 3.2. Growth rates

219 Because the shell growth rate of oysters is not constant, even at a same site (Richardson et al.,
220 1993; Lartaud et al., 2010b), the distribution of Mn-markings throughout the hinge is highly
221 variable from one shell to another. Using the markings as time limits, the seasonal growth
222 rates have been estimated for each shell assuming a constant growth rate between consecutive
223 markings (Table 3). The seasonal growth rates of the juvenile *Crassostrea gigas* specimens
224 range from 5.6 to 27.4 $\mu\text{m}/\text{day}$, with the highest values obtained on the shells collected at the
225 Baie des Veys station. The growth rates measured for adult *C. gigas* (only from the

226 Marennnes-Oléron location) range from 2.0 to 7.4 $\mu\text{m}/\text{day}$. The adult shells of *Ostrea edulis*
227 show growth rates ranging from 2.0 to 10.7 $\mu\text{m}/\text{day}$, depending on the season. As for juvenile
228 *C. gigas*, higher growth rates of *O. edulis* are obtained for specimens bred at the Baie des
229 Veys station.

230

231 Table 3

232

233 3.3. Mg/Ca evolution in oyster shells

234 3.3.1. At Baie des Veys (Table 4)

235 All of the spots of the analysed profile of the juvenile *C. gigas* shells are located in the part of
236 the hinge corresponding to the experimental period. The profiles start between June 2005 and
237 September 2005 (Fig. 4a) and end on the collection day, in November 2006. The Mg/Ca ratios
238 in the juvenile *C. gigas* shells range from 0.87 to 9.92 mmol/mol and show similar trends. The
239 highest Mg/Ca ratios correspond to the summer months (April to October), while lower
240 Mg/Ca ratios are obtained during the winter months (November to March, Fig. 4a). Because
241 of the short period of the Mn-marking experiment for the adult *O. edulis*, we have retained
242 only the relevant geochemical data (i.e., those obtained between the reliable markings, Fig.
243 4c). The Mg/Ca ratios recorded in adult *O. edulis* shells are slightly lower than those in the
244 juvenile *C. gigas* (range between 0.84 and 8.07 mmol/mol, Table 4), and they increase
245 slightly until the collection day.

246

247 Table 4

248 Figure 4

249

250 3.3.2. At Marennnes-Oléron (Table 4)

251 As shown before, the growth rates of the oysters bred at Marennes-Oléron are half of those
252 bred at Baie des Veys. Moreover, when the oysters reached an age of two years, their growth
253 rates decreased consistently. For these two reasons, the sampling resolution after time
254 calibration was much lower, implying that the geochemical interpretations at Baie des Veys
255 became more uncertain, especially with regards to adult specimens. The Mg/Ca ratios of the
256 juvenile *C. gigas* shells exhibit values ranging from 1.27 to 10.51 mmol/mol (mean $4.14 \pm$
257 1.54 mmol/mol), and the highest Mg/Ca ratios were recorded during the summer period. The
258 Adult *C. gigas* shells (Fig. 4b, grey lines) yielded higher mean values (4.82 ± 2.06 mmol/mol
259 and 7.10 ± 1.68 mmol/mol) and wider amplitudes (from 1.25 to 16.60 mmol/mol, Table 4).
260 Similar to the Baie des Veys shells, the very low growth rate of the adult *O. edulis* shells at
261 Marennes-Oléron bias the high-resolution investigation of the Mg/Ca ratios, with one point
262 corresponding to 15 days at best (Fig. 4d). The Mg/Ca ratios in the adult *O. edulis* shells show
263 the highest values of all of the samples, with a range between 3.25 and 17.57 mmol/mol
264 (Table 4). However, the mean values (mean 5.13 ± 1.87 mmol/mol and 6.84 ± 3.02
265 mmol/mol) are similar to those from the adult *C. gigas*. Finally, no clear trend is conspicuous
266 during the time interval analysed.

267

268 **4. Discussion**

269 *4.1. Shell growth analysis*

270 Taking into account all samples, oyster shell growth rates vary seasonally. Higher growth
271 rates are observed during summer (with a mean value of $16.1 \mu\text{m/day}$) than winter (with a
272 mean value of $11.5 \mu\text{m/day}$, Table 3) except for the specimen jn-gigBV-1. The fact that shell
273 deposition is clearly visible between all winter markings confirms that, as previously reported
274 by Lartaud et al. (2010b), *Crassostrea gigas* shell mineralisation can occur at both sites
275 during cold months. During this period, no evidence of growth line (so called winter line) or

276 annual growth break can be revealed as this can be done on other bivalve shells (Schöne et al.,
277 2004). These results differ from those of the eastern oyster *Crassostrea virginica*, which
278 undergoes growth breaks when temperatures fall below 10°C (Kirby et al., 1998). An
279 ontogenetic trend is observed that leads to lower growth performance in adult shells. Because
280 *Ostrea edulis* grew only from February 2006 to November 2006 in Marennes-Oléron and
281 from March 2006 to November 2006 in the Baie des Veys, the winter estimates of the growth
282 rate are not available for this study. However, the two adult species cultured at Marennes-
283 Oléron show that the *C. gigas* shells grow almost twice as fast as *O. edulis* (7.7 vs. 3.5
284 $\mu\text{m/day}$). Additionally, regardless of their species, the oysters at Baie des Veys grow faster
285 (mean 12.5 $\mu\text{m/day}$) than those from Marennes-Oléron (mean 5.6 $\mu\text{m/day}$).

286

287 4.2. Shell Mg/Ca ratios and ontogeny in short-lived oysters

288 The use of metal-to-calcium ratios in bivalve shells as paleothermometers, unlike its use in
289 other taxa such as foraminifera or corals, is still poorly documented. Stecher et al. (1996) and
290 Carré et al. (2006) described a positive ontogenetic trend of Mg incorporation in the shells of
291 various clam species. These observations contrast with the results from Strasser et al. (2008)
292 concerning *Mya arenaria* and Higuera-Ruiz and Elorza (2009) for *C. gigas*, who noted a
293 decrease in the Mg incorporation with size. Other studies have emphasised the correlations
294 between the shell Mg record and its growth rate (Takesue and van Geen, 2004) or age (Freitas
295 et al., 2005). Although the investigation of an ontogenetic trend is difficult because of the
296 short life span of the specimens used in the present study, juvenile *C. gigas* from both sites
297 exhibit similar Mg/Ca ratios between six months and two years-old, whereas an increase in
298 the Mg/Ca ratio is recorded for adult *C. gigas* shells (i.e., ages between two and a half and
299 three years, Table 4).

300 The Mg/Ca records of the two species between the two breeding sites are slightly different,
301 with chemical ratios higher in the shells from Marennes-Oléron. These differences are closely
302 linked to the seawater Mg/Ca ratios of the sites (Table 2). Furthermore, adult *C. gigas* and *O.*
303 *edulis* shells cultured at the same site exhibit similar Mg/Ca ratios, suggesting that the
304 species-related ‘vital effect’ is weak and that it does not significantly influence the Mg
305 incorporation into the carbonate lattice of those oysters. A similar result was reported for $\delta^{18}\text{O}$
306 by Kirby et al. (1998).

307

308 *4.3. High frequency Mg/Ca variation in oyster shells*

309 The Mg/Ca evolution in shells shows different cyclicities. Because this work focuses on the
310 use of the calcite Mg/Ca molar ratio as a paleothermometer for seasonal contrast estimations,
311 it is imperative to determine the origin of these cyclicities (i.e., environmental control or
312 analytical bias). The FFT performed on the Mg/Ca record of all the shells reveals two main
313 cyclicities. Two main ranges of periodicity (13.7 to 15,4 and 25.6 to 31.3 solar days) are
314 identified in both sites for all juvenile oysters, while nothing can be seen on the adult
315 specimens because of the weakness of the sampling resolution for the studied time span
316 (except for ad-edu-BV-1, Table 5). Based on the sclerochronological approaches, these types
317 of periodicities have been already identified on mollusc bivalve shells and related to tidal
318 cycles (Evans, 1972; Pannella, 1976; Higuera-Ruiz and Elorza, 2009; Lartaud et al., 2010a).
319 The reported lunar calendar shows that the Mg/Ca ratio is higher during full-moon spring
320 tides and lower during new-moon spring tides (Fig. 5). Surprisingly, Higuera-Ruiz and Elorza
321 (2009) show the opposite result, with a lower Mg/Ca ratio during a single spring tide (without
322 any distinction between the new or full-moon spring tide) in an oyster shell from the Bay of
323 Biscay (Spain). Based on the relationship between the shell Mg/Ca ratio and the temperature
324 (Lerman, 1965; Vander Putten et al., 2000; Freitas et al., 2009), the authors attributed this

325 fortnightly pattern to the input of cold water during the spring tides. However, evidence of
326 such a temperature changes with the tide is not observed in either Baie des Veys or Marennes-
327 Oléron. Parameters other than the temperature have been reported to modify the Mg
328 concentration in the shells, such as metabolically controlled processes that lead to variations
329 in Mg in the organic matrix (Vander Putten et al., 2000; Takesue et al., 2008). The primary
330 energy provider in all organisms is adenosine triphosphate (ATP). The formation of this
331 molecule mainly derives from the catabolism of carbohydrates. The reactions that use ATP
332 require Mg^{2+} as a cofactor. This requirement leads, for example, to nycthemeral changes in
333 the uptake of Mg^{2+} (Lazareth et al., 2007). Tides are recognised as environmental pacemakers
334 for endogenous timekeeping mechanisms, the so-called biological clocks (Richardson, 1996;
335 Schöne, 2008), and metabolic control of the Mg concentration in the organic matrix that
336 depends on spring (new-moon or full-moon) and neap tides cannot be precluded.

337

338 Figure 5, Table 5

339

340 4.4. Mg/Ca vs seawater temperature (SST)

341 The seasonal variation of the Mg/Ca ratios in bivalve shells is not linked to changes in the
342 seawater Mg/Ca ratio for salinities greater than 10 psu (Dodd and Crisp, 1982). However, in
343 estuarine environments, the seawater Mg/Ca ratio can vary significantly over a salinity range
344 from 10 to 37 psu (Surge and Lohmann, 2008). In this study, because salinity remains fairly
345 constant at approximately 33 psu in both locations (see § 3.1), changes in the seawater Mg/Ca
346 ratio should be low throughout the year. Highly significant good correlations ($r = 0.55$, $p <$
347 0.0001) to high correlations ($0.70 < r < 0.83$, $p < 0.0001$) between the SST and the Mg/Ca
348 ratio have been observed for juvenile *C. gigas* shells from both Baie des Veys and Marennes-
349 Oléron (Fig. 6). The Mg/Ca ratios of the two adult specimens of *C. gigas* from Marennes-

350 Oléron show conflicting results, with negative and positive correlations ($r = -0.24$ for ad-gig-
351 MO-2 and $r = 0.73$ for ad-gig-MO-3). It is remarkable that the positive correlation
352 corresponds to the shell with the higher growth rate, especially in summer (Table 3). For *O.*
353 *edulis* shells, the correlations are weak to absent ($-0.1 < r < 0.47$) at Baie des Veys, according
354 to the shell growth performance (Table 3), and negative correlations are observed at
355 Marennes-Oléron ($r = -0.80$ and $r = -0.36$, Fig. 5), where the shell growth rate is low (Table
356 3). These results suggest that the Mg/Ca ratio in the shells is correlated with the seawater
357 temperature only when growth rate is high. At low growth rates, metabolic/kinetic effects
358 appear to control metal incorporation into the shells. This control is linked to calcium
359 selectivity against magnesium, which complicates the environmental Mg/Ca relationship
360 (Vander Putten et al., 2000; Schöne et al., 2011).

361 When the SST-Mg/Ca relationship is significant (e.g., for juvenile shells), Mg and Ca exhibit
362 different pathways in different seasons. In the same temperature range, the shell Mg/Ca ratios
363 are lower when the seasonal SST trend decreases (autumn) and higher when it increases
364 (spring). Considered separately, the Mg/Ca-temperature relationships can be described by two
365 slightly different equations, which have higher correlation coefficients than the global set of
366 data. Because the temperature range is the same for both seasonal data sets, these results may
367 reflect the impact of metabolic effects on the incorporation of Mg/Ca in the shell.

368

369 Figure 6

370

371 A Mg/Ca-temperature equation has been calculated from the Mg/Ca ratios of juvenile oyster
372 shells from both sites, with one exception: shell jn-gig-BV-1. The Mg/Ca evolution curve
373 from this individual does not follow the same pattern as that of the other specimens, with
374 depleted values between July and August 2006 and anomalously increasing ratios during the

375 last autumn. Nevertheless, the CL age model remains in correlation with the effective
376 seasonal periods. This result implies that Mg/Ca evolution in the jn-gig-BV-1 shell is not
377 based on temperature variations but rather to stress or illness during experiment. Excluding
378 this irrelevant datum from the complete juvenile Mg/Ca data set, the calculated Mg/Ca-
379 temperature linear relationship is given by the following expression:

$$380 \quad T = 3.77Mg/Ca + 1.88 \quad (1)$$

381 where T is the temperature in °C and Mg/Ca is the elemental ratio of the juvenile *C. gigas*
382 shells (in mmol/mol).

383

384 This equation differs from the one obtained for *C. virginica* by Surge and Lohmann (2008):

$$385 \quad T = 1.39Mg/Ca + 0.23 \quad (2).$$

386 Beyond the fact that the studied species is different, the main
387 differences between their work and the present study concern the environment of the living

388 oysters. During their experiments (conducted in the Gulf of Mexico), Surge and Lohmann

389 recorded seawater temperatures ranging from 19.6 to 31.6 °C and salinity ranging from 7.9 to

390 38.5 psu. Furthermore, these authors described a poor correlation between the temperature

391 and the shell Mg/Ca because of an ontogenetic effect that influenced the incorporation of Mg

392 into the *C. virginica* shell during the first years of growth. They also observed a decrease of

393 the accuracy of date assignments further back in the geochemical record. The most accurate

394 equation was finally obtained using the geochemical data corresponding to the most recent

395 part of the adult shells. Klein et al. (1996) demonstrated that the Mg/Ca ratio from the calcitic

396 part of *M. edulis* is well correlated with the SSTs, and they proposed the following overall

397 equation: $T = 3.33Mg/Ca - 7.5$ (3). During their experiment, the mussels were grown at

398 Squirrel Cove (British Columbia, Canada), where the SSTs were between 6.1 and 22.7°C,

399 which is very similar to the temperature range of the present study. Figure 7 depicts the

comparison of the calculated SSTs using the different models with the measured seawater

400 temperatures. The geochemical data used for the temperature calculation are those of the three
401 selected juvenile *C. gigas* shells from both sites. The estimated SSTs obtained using the
402 Equation 2 and the Equation 3 underestimate the seawater temperatures by approximately ten
403 degrees (with some negative temperatures during the winter months). In detail, the calculated
404 temperatures determined from the equation of Surge and Lohmann (2008) smooth the
405 sinusoidal shape of the temperature curve, with a seasonal variation of less than 6-7°C. The
406 comparison of our temperature estimates with the one calculated by the method of Klein et al.
407 (1996) suggests that the Mg incorporation differs between the *M. edulis* and *C. gigas* shells,
408 and thus that an inter-specific calibration is necessary for paleoclimatic investigations. In
409 contrast, *C. virginica* and *C. gigas* are closely related species, but the experiments were
410 carried out in significantly different environments. The Surge and Lohmann equation is
411 suitable for high temperatures and variable salinities; therefore, it is most likely not valid for
412 the French temperate environments.

413

414 Figure 7

415

416 **6. Conclusion**

417 In this study, an electron microprobe Mg/Ca analysis was performed on *Crassostrea gigas*
418 and *Ostrea edulis* shells. The animals were bred over two years in two different locations on
419 the French Atlantic coast, where the seawater salinities and temperatures were recorded daily.
420 The shells were marked monthly using Mn-doped seawater. After collection, chemical
421 markings were used to time-calibrate the Mg/Ca shell profiles with daily precision.
422 Frequency analysis of the chemical records shows that the high frequency variation is well
423 synchronised with the spring tides, suggesting that Mg incorporation into the shell is partly
424 influenced by physiological processes. Furthermore, ontogenetic processes strongly affect

425 Mg/Ca incorporation into the adult shells, preventing any available correlation with the
426 seawater temperature. On the seasonal scale, a highly significant correlation is observed
427 between the Mg/Ca ratios and the seawater temperatures, especially in regard to the *C. gigas*
428 juvenile specimens. Using data from the two study sites, an overall relationship between the
429 Mg/Ca shell ratios and the seawater temperatures is given by the following equation:
430 $T = 3.77Mg/Ca + 1.88$ (T in °C and Mg/Ca in mmol/mol). The comparison with previously
431 published equations highlights the potential of *Crassostrea gigas* shell Mg/Ca variations for
432 seasonal temperature estimations in temperate environments.

433

434 **Acknowledgements**

435 This work was supported by the INTERRVIE program of the Centre National de la
436 Recherche Scientifique (CNRS) and the Pierre et Marie Curie University. Authors are grateful
437 to P. Geairon and S. Robert (IFREMER, Marennes-Oléron) and M. Ropert, F. Rauflet and A.
438 Gangnery (IFREMER, Port-en-Bessin) for their advices and for material/technical assistance
439 during oyster farming. *Crassostrea aginensis* fossils were provided by C. Cavelier (BRGM,
440 Orléans). We are also grateful to S. Boulila (UPMC) for his help on signal processing. We
441 would like to thank Alberto Pérez-Huerta and the two anonymous reviewers for
442 constructive comments and the guest editors for inviting us to contribute to this
443 special issue and for their work in preparing it.

444

445 **References**

446 Andreasson, F.P., Schimtz, B., 2000. Temperature seasonality in the early middle Eocene
447 North Atlantic region: evidence from stable isotope profiles of marine gastropod shells. Geol.
448 Soc. Am. Bull. 112, 628-640.

449 Boulila, S., Galbrun, B., Hinnov, L.A., Collin, P.-Y., 2008. High-resolution cyclostratigraphic
450 analysis from magnetic susceptibility in a Lower Kimmeridgian (Upper Jurassic) marl-
451 limestone succession (La Méouge, Vocontian Basin, France). *Sediment. Geol.* 203, 54-63.

452 Boyden, C.R., Phillips, D.J.H., 1981. Seasonal variation and inherent variability of trace
453 elements in oysters and their implications for indicator studies. *Mar. Ecol. Prog. Ser.* 5, 29-40.

454 Carré, M., Bentaleb, I., Bruguier, O., Ordinola, E., Barrett, N.T., Fontugne, M., 2006.
455 Calcification rate influence on trace element concentrations in aragonitic bivalve shells:
456 evidences and mechanisms. *Geochim. Cosmochim. Acta* 70, 4906–4920.

457 Cronblad, H.G., Malmgren, B.A., 1981. Climatically controlled variation of Sr and Mg in
458 Quaternary planktonic foraminifera. *Nature* 291, 61-64.

459 Dodd, J.R., 1965. Environmental control of strontium and magnesium in *Mytilus*. *Geochim.*
460 *Cosmochim. Acta* 29, 385-398.

461 Dodd, J.R., Crisp, E.L., 1982. Non-linear variation with salinity of Sr/Ca and Mg/Ca ratios in
462 water and aragonitic bivalve shells and implications for paleosalinity studies. *Palaeogeogr.,*
463 *Palaeoclimatol., Palaeoecol.* 38, 45-56.

464 England, J., Cusack, M., Lee, M.R., 2007. Magnesium and sulphur in the calcite shells of two
465 brachiopods, *Terebratulina retusa* and *Novocrania anomala*. *Lethaia* 40, 2-10.

466 Epstein, S., Mayeda, T., 1953. Variation of ¹⁸O content of waters from natural sources.
467 *Geochim. Cosmochim. Acta* 4, 213-224.

468 Evans, J.W., 1972. Tidal growth increments in the cockle *Clinocardium nuttalli*. *Science* 176,
469 416-417.

470 Freitas, P., Clarke, L.J., Kennedy, H., Richardson, C., Abrantes, F., 2005. Mg/Ca, Sr/Ca, and
471 stable-isotope ($\delta^{18}\text{O}$ and $\delta^{13}\text{C}$) ratio profiles from the fan mussel *Pinna nobilis*: seasonal
472 records and temperature relationships. *Geochem., Geophys., Geosyst.* 6. doi:
473 10.1029/2004GC000872.

474 Freitas, P.S., Clarke, L.J., Kennedy, H., Richardson, C.A., Abrantes, F., 2006. Environmental
475 and biological controls on elemental (Mg/Ca, Sr/Ca and Mn/Ca) ratios in shells of the king
476 scallop *Pecten maximus*. *Geochim. Cosmochim. Acta* 70, 5119-5133.

477 Freitas, P.S., Clarke, L.J., Kennedy, H., Richardson, C.A., 2009. Ion microprobe assessment
478 of the heterogeneity of Mg/Ca, Sr/Ca and Mn/Ca ratios in *Pecten maximus* and *Mytilus edulis*
479 (bivalvia) shell calcite precipitated at constant temperature. *Biogeosci. Disc.* 6, 1267-1316.

480 Gillikin, D.P., De Ridder, F., Ulens, H., Elskens, M., Keppens, E., Baeyens, W., Dehairs, F.,
481 2005. Assessing the reproductibility and reliability of estuarine bivalve shells (*Saxidomus*
482 *giganteus*) for sea surface temperature reconstruction: Implications for paleoclimate studies.
483 *Palaeogeogr., Palaeoclimatol., Palaeoecol.* 228, 70-85.

484 Hawkes, G.P., Day, R.W., Wallace, M.W., Nugent, K.W., Bettioli, A.A., Jamieson, D.N.,
485 1996. Analysing the growth and form of molluscs shell layers *in situ*, by
486 cathodoluminescence microscopy and Raman spectroscopy. *J. Shellfish Res.* 15, 659-666.

487 Higuera-Ruiz, R., Elorza, J., 2009. Biometric, microstructural, and high-resolution trace
488 element studies in *C. gigas* of Cantabria (Bay of Biscay, Spain): Anthropogenic and seasonal
489 influences. *Estuar. Coast. Shelf Sci.* 82, 201-213.

490 Immenhauser, A., Nägler, T.F., Steuber, T., Hippler, D., 2005. A critical assessment of
491 mollusc $^{18}\text{O}/^{16}\text{O}$, Mg/Ca, and $^{44}\text{Ca}/^{40}\text{Ca}$ ratios as proxies for Cretaceous seawater temperature
492 seasonality. *Palaeogeogr., Palaeoclimatol., Palaeoecol.* 215, 221-237.

493 Kaehler, S., McQuaid, I.R., 1999. Use of the fluorochrome calcein as an *in situ* growth
494 marker in the brown mussel *Perna perna*. *Mar. Biol.* 133, 455-460.

495 Kirby, M.X., Soniat, T.M., Spero, H.J., 1998. Stable isotope sclerochronology of Pleistocene
496 and recent oyster shells (*Crassostrea virginica*). *Palaios* 13, 560-569.

497 Klein, R.T., Lohmann, K.C., Thayer, C.W., 1996. Bivalve skeletons record seas-surface
498 temperature and $\delta^{18}\text{O}$ via Mg/Ca and $^{18}\text{O}/^{16}\text{O}$ ratios. *Geology* 24, 415-418.

499 Langlet, D., Alunno-Bruscia, M., de Raféelis, M., Renard, M., Roux, M., Schein, E., Buestel,
500 D., 2006. Experimental and natural cathodoluminescence in the shell of *Crassostrea gigas*
501 from Thau lagoon (France): ecological and environmental implications. *Mar. Ecol. Prog. Ser.*
502 317, 143-156.

503 Lartaud, F., Langlet, D., de Raféelis, M., Emmanuel, L., Renard, M., 2006. Mise en évidence
504 de rythmicité saisonnière dans la coquille des huîtres fossiles *Crassostrea aginensis*,
505 Tournouer, 1914 (Aquitaniens) et *Ostrea bellovacina*, Lamarck, 1806 (Thanétien). Approche
506 par cathodoluminescence et sclérochronologie. *Geobios* 39, 845-852.

507 Lartaud, F., Chauvaud, L., Richard, J., Toulot, A., Bollinger, C., Testut, L., Paulet, Y.M.,
508 2010a. Experimental growth pattern calibration of Antarctic scallop shells (*Adamussium*
509 *colbecki*, Smith 1902) to provide a biogenic archive of high-resolution records of
510 environmental and climatic changes. *J. Exp. Mar. Biol. Ecol.* 393, 158-167.

511 Lartaud, F., de Raféelis, M., Ropert, M., Emmanuel, L., Geairon, P., Renard, M., 2010b. Mn
512 labelling of living oysters: Artificial and natural cathodoluminescence analyses as a tool for
513 age and growth rate determination of *C. gigas* (Thunberg, 1793) shells. *Aquaculture* 300, 206-
514 217.

515 Lartaud, F., Emmanuel, L., de Raféelis, M., Ropert, M., Labourdette, N., Richardson, C.A.,
516 Renard, M., 2010c. A latitudinal gradient of seasonal temperature variation recorded in oyster
517 shells from the coastal waters of France and The Netherlands. *Facies* 56, 13-25.

518 Lazareth, C.E., Vander Putten, E., André, L., Dehairs, F., 2003. High-resolution trace element
519 profiles in shells of the mangrove bivalve *Isognomon ephippium*: a record of environmental
520 spatio-temporal variations? *Estuar. Coast. Shelf Sci.* 57, 1103-1114.

521 Lazareth, C.E., Guzman, N., Poitrasson, F., Candaudap, F., Ortlieb, L., 2007. Nyctemeral
522 variations of magnesium intake in the calcitic layer of a Chilean mollusk shell (*Concholepas*
523 *concholepas*, Gastropoda). *Geochim. Cosmochim. Acta* 71, 5369-5383.

524 Lerman, A. 1965. Strontium and magnesium in water and in *Crassostrea* calcite. Science 150,
525 745-751.

526 Mahe, K., Bellamy, E., Lartaud, F., de Rafelis, M., 2010. Calcein and manganese experiments
527 for marking the shell of the common cockle (*Cerastoderma edule*): tidal rhythm validation of
528 increments formation. Aquat. Living Resour. 23, 239-245.

529 Paillard, D., Labeyrie, L., Yiou, P., 1996. Macintosh program performs time-series analysis.
530 Eos Trans. AGU, 77-379.

531 Pannella, G., 1976. Tidal growth patterns in recent and fossil mollusc bivalve shells: a tool for
532 the reconstruction of paleotides. Naturwissenschaften 63, 539-543.

533 Richardson, C.A., 1996. Exogenous or endogenous control of growth band formation in
534 subtidal bivalve shells? Bull. Inst. Oceanogr. (Monaco) 14, 133-141.

535 Richardson, C.A., Collis, S.A., Ekaratne, K., Dare, P., Key, D., 1993. The age determination
536 and growth rate of the European flat oyster, *Ostrea edulis*, in British waters determined from
537 acetate peels of umbo growth lines. ICES J. Mar. Sci. 50, 493-500.

538 Rohling, E.J., 2000. Paleosalinity: confidence limits and future applications. Mar. Geol. 163,
539 1-11.

540 Schöne, B.R., Oschmann, W., Tanabe, K., Dettman, D., Fiebig, J., Houk, S.D., Kanie, Y.,
541 2004. Holocene seasonal environmental trends at Tokyo Bay, Japan, reconstructed from
542 bivalve mollusk shells-implications for changes in the East Asian monsoon and latitudinal
543 shifts of the Polar Front. Quat. Sci. Rev. 23, 1137-1150.

544 Schöne, B.R., 2008. The curse of physiology-challenges and opportunities in the
545 interpretation of geochemical data from mollusk shells. Geo-Mar Lett. 28, 269-285.

546 Schöne, B.R., Zhang, Z., Radermacher, P., Thébault, J., Jacob, D.E., Nunn, E.V., Maurer, A.-
547 F., 2011. Sr/Ca and Mg/Ca ratios of ontogenetically old, long-lived bivalve shells (*Arctica*

548 *islandica*) and their function as paleotemperature proxies. *Palaeogeogr., Palaeoclimatol.,*
549 *Palaeoecol.* 302, 52-64.

550 Stecher, H.A., Krantz, D.E., Lord III, C.J., Luther III, G.W., Bock, K.W., 1996. Profiles of
551 strontium and barium in *Mercenaria mercenaria* and *Spisula solidissima* shells. *Geochim.*
552 *Cosmochim. Acta* 60, 3445–3456.

553 Stenzel, H.B., 1971. Oysters, in: Moore, R.C. (Eds.), *Treatise in Invertebrate Paleontology,*
554 *Mollusca 6, Bivalvia.* Boulder, Colorado & Lawrence, Kansas: Geol. Soc. Amer. &
555 University of Kansas Press 3, 953-1197.

556 Strasser, C.A., Mullineaux, L.S., Walther, B.D., 2008. Growth rate and age effects on *Mya*
557 *arenaria* shell chemistry: implications for biogeochemical studies. *J. Exp. Mar. Biol. Ecol.*
558 355, 153–163.

559 Surge, D., Lohmann, K.C., 2008. Evaluating Mg/Ca ratios as a temperature proxy in the
560 estuarine oyster, *Crassostrea virginica*. *J. Geophys. Res.*, G02001, doi:
561 10.1029/2007JG000623.

562 Takesue, R.K., van Geen, A., 2004. Mg/Ca, Sr/Ca, and stable isotopes in modern and
563 Holocene *P. staminea* shells from a northern California coastal upwelling region. *Geochim.*
564 *Cosmochim. Acta* 68, 19, 3845-3861.

565 Takesue, R.K., Bacon, C.R., Thompson, J.K., 2008. Influences of organic matter and
566 calcification rate in trace elements in aragonitic estuarine bivalve shells. *Geochim.*
567 *Cosmochim. Acta* 72, 5431-5445.

568 Thomson, D.J., 1982. Spectrum estimation and harmonic analysis. *IEEE Proc.* 70, 1055-1096.

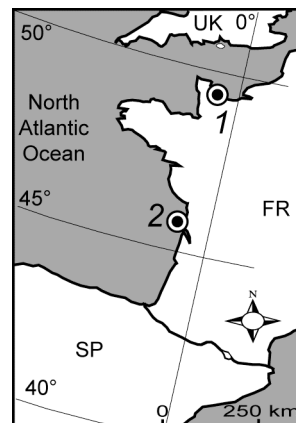
569 Vander Putten, E., Dehairs, F., Keppens, E., Baeyens, W., 2000. High resolution distribution
570 of trace elements in the calcite shell layer of modern *Mytilus edulis*: environmental and
571 biological controls. *Geochim. Cosmochim. Acta* 64, 997–1011.

572 Wisshak, M., Lopez Correa, M., Gofas, S., Salas, C., Taviani, M., Jakobsen, J., Freiwald, A.,
573 2009. Shell architecture, element composition, and stable isotope signature of the giant deep-
574 sea oyster *Neopycnodonte zibrowii* sp. N. from the NE Atlantic. Deep-sea Research 56, 374-
575 407.

576

577 **Figure**

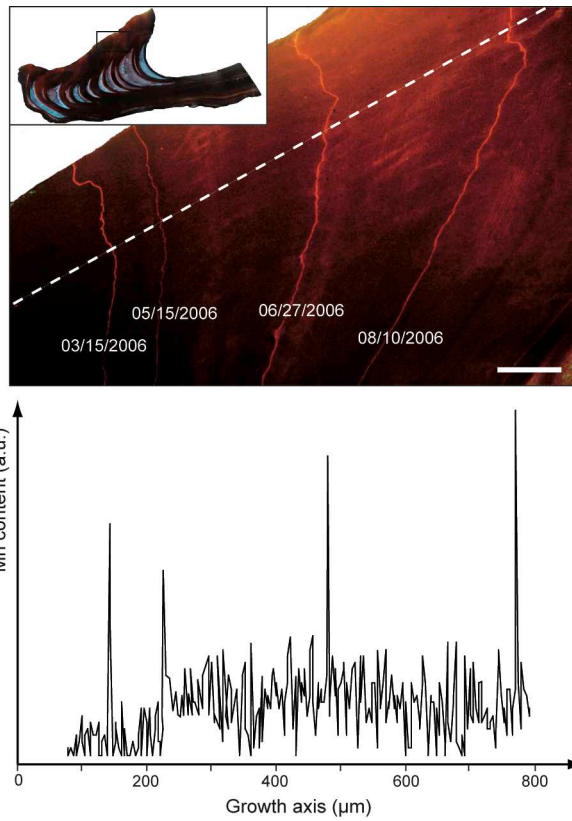
578 Figure 1: Location map of the studied breeding sites: French oyster farming of (1) Baie des
579 Veys (Normandy) and (2) Marennes-Oléron (Charente-Maritime).



580

581

582 Figure 2: Cathodoluminescence microphotograph of oyster shell section showing both natural
583 luminescence and bright luminescent bands corresponding to the Mn-marking days. White
584 dashed line represents the electron microprobe transect along which the measurements were
585 taken along the hinge region (scale bar is 200 μ m). The graph beneath shows the relative Mn
586 profile along the transect (a.u. = arbitrary unit) where each Mn Marking (bright luminescent
587 increment) corresponds with high Mn content.

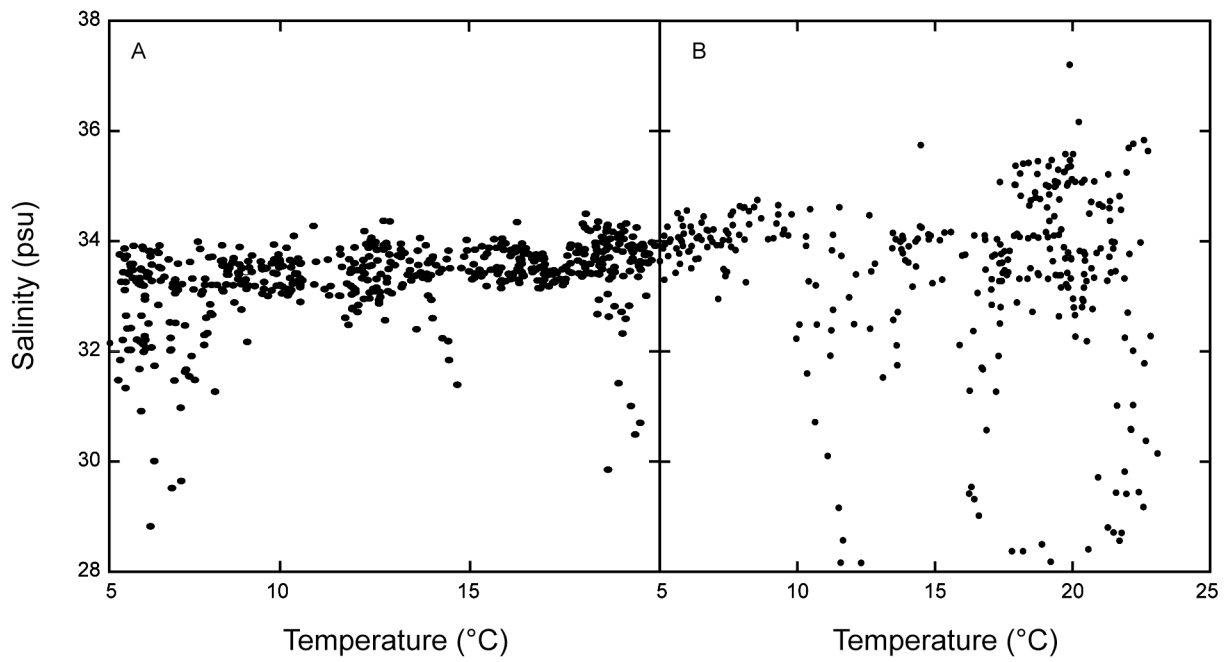


588

589

590 Figure 3 : Measured seawater salinity and temperature in both locations : A- Baie des Veys,

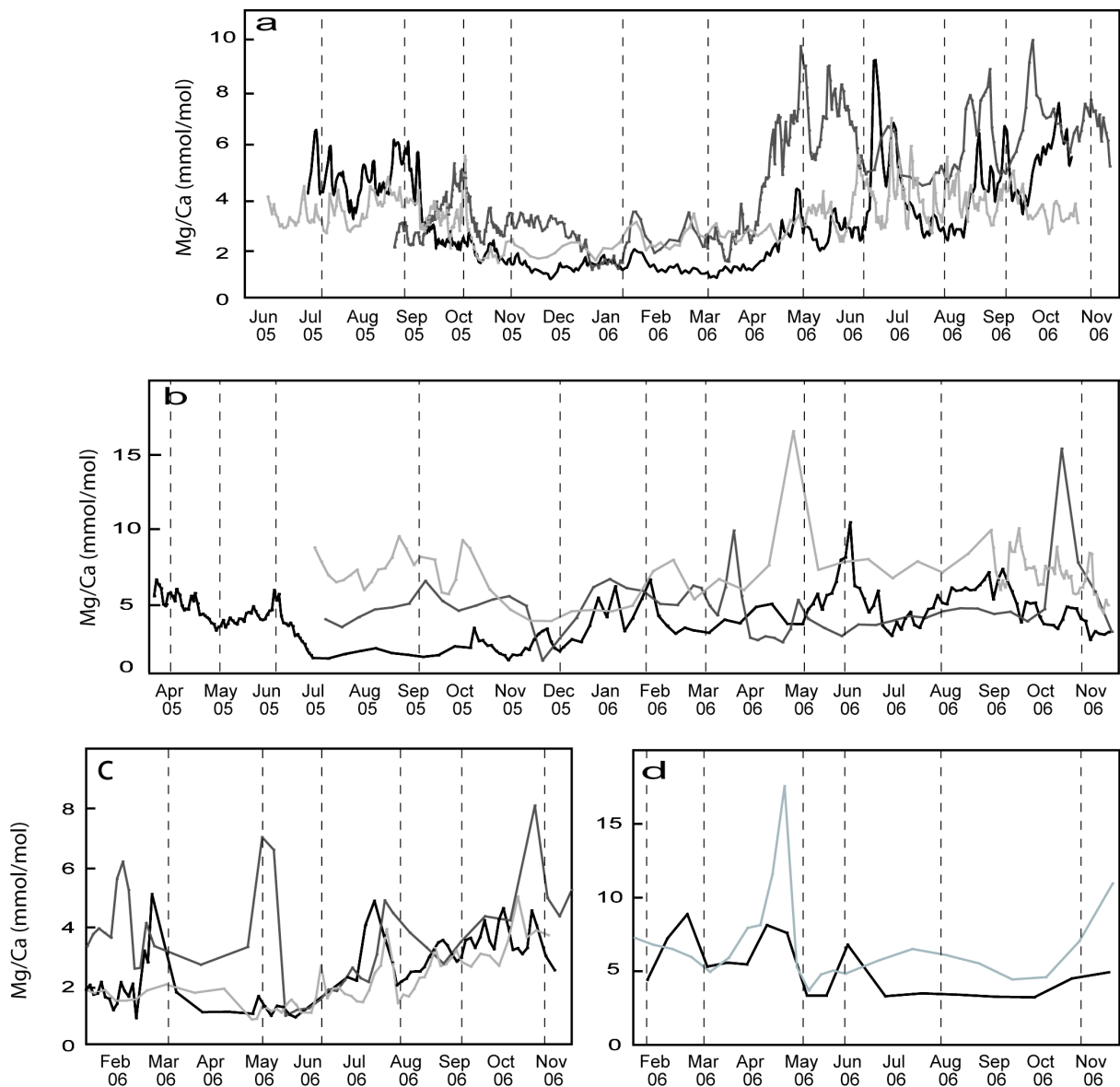
591 B- Marennes-Oléron.



592

593

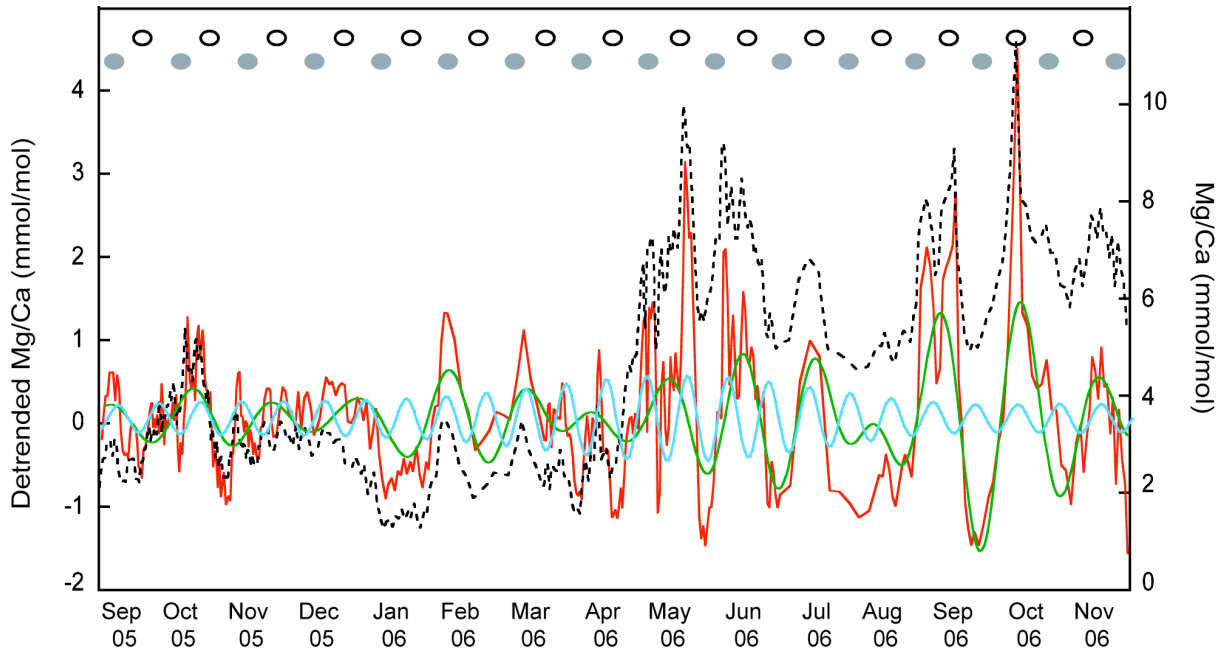
594 Figure 4: Electron microprobe Mg/Ca evolution curve of the studied osyter shells (hinge
 595 region). All curves are time calibrated using monthly Mn-markings. a- juvenile *C. gigas* shells
 596 from Baie des Veys: jn-gig-BV-1 (dark grey line, n= 394), jn-gig-BV-2 (black line, n=394),
 597 jn-gig-BV-3 (light grey line, n=398); b- juvenile and adult *C. gigas* shells from Marennes-
 598 Oléron: jn-gig-MO-1 (black line, n=190), ad-gig-MO-2 (dark grey line, n=54), ad-gig-MO-3
 599 (light grey line, n= 96); c- adult *O. edulis* shells from Baie des Veys: ad-edu-BV-1 (black line,
 600 n=67), ad-edu-BV-2 (dark grey line, n=39), ad-edu-BV-3 (light grey line, n=59); d- adult *O.*
 601 *edulis* shells from Marennes-Oléron: ad-edu-MO-1 (black line, n=18), ad-edu-MO-2 (light
 602 grey line, n=23). The vertical dashed lines correspond to Mn-marking days.



603

604

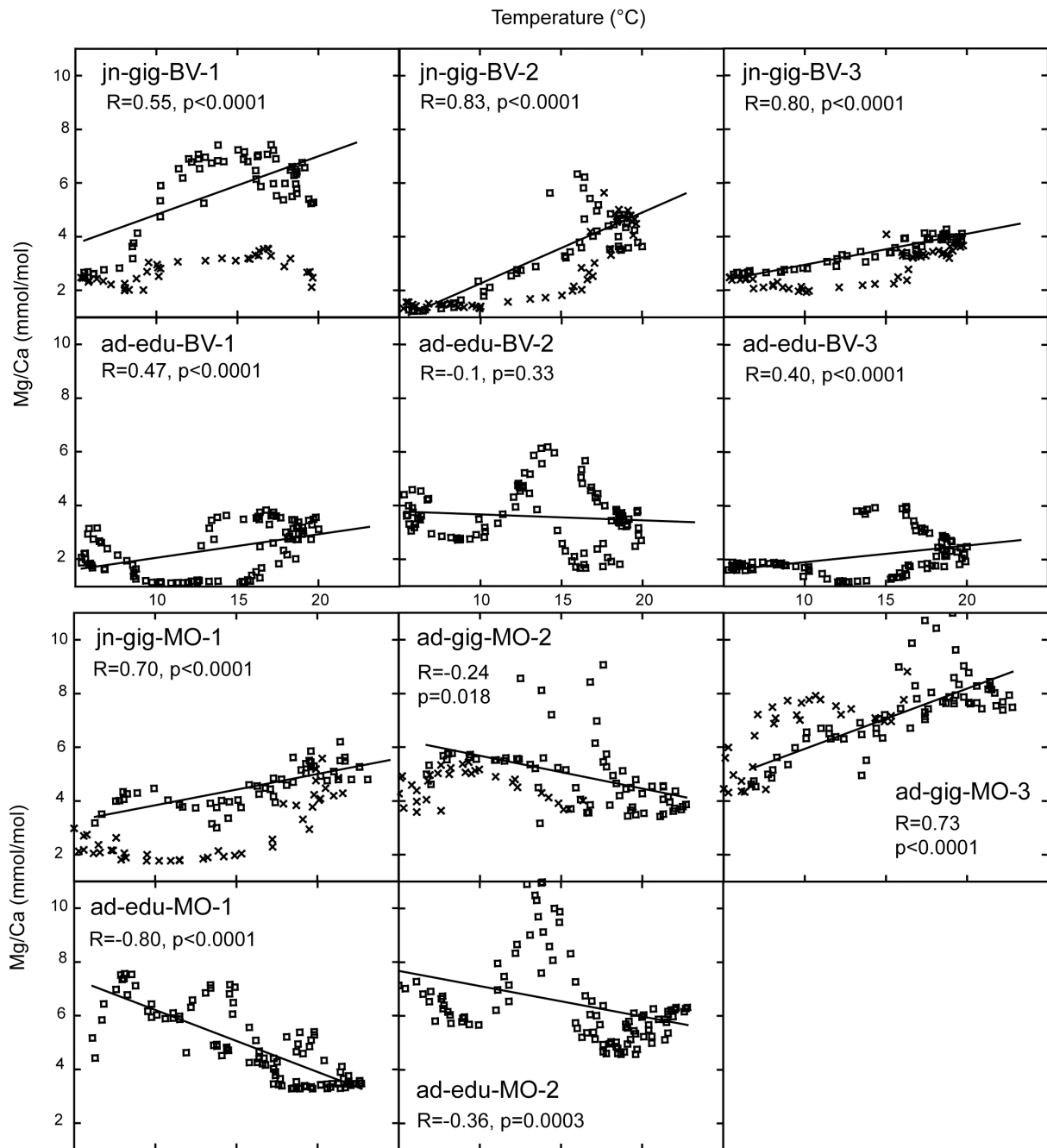
605 Figure 5: Shell Mg/Ca evolution curve (dashed black line), detrended Mg/Ca curve (red line)
606 compared with a 28-days cycles (green line) and with a 14-days cycles (blue line). New moon
607 spring tides (grey circles) and full moon spring tides (white circles) are indicated.



608

609

610 Figure 6: Smoothed Mg/Ca ratios plotted versus seawater temperature. Correlation
611 coefficients R are obtained using a simple linear regression. Square symbols are Mg/Ca ratios
612 corresponding to the increasing temperatures (spring to summer) and cross symbols the
613 Mg/Ca ratios during the decreasing temperatures (autumn to winter).



614

615

616 Figure 7: Seawater temperatures calculated from Mg/Ca ratios in juvenile *C. gigas* shells

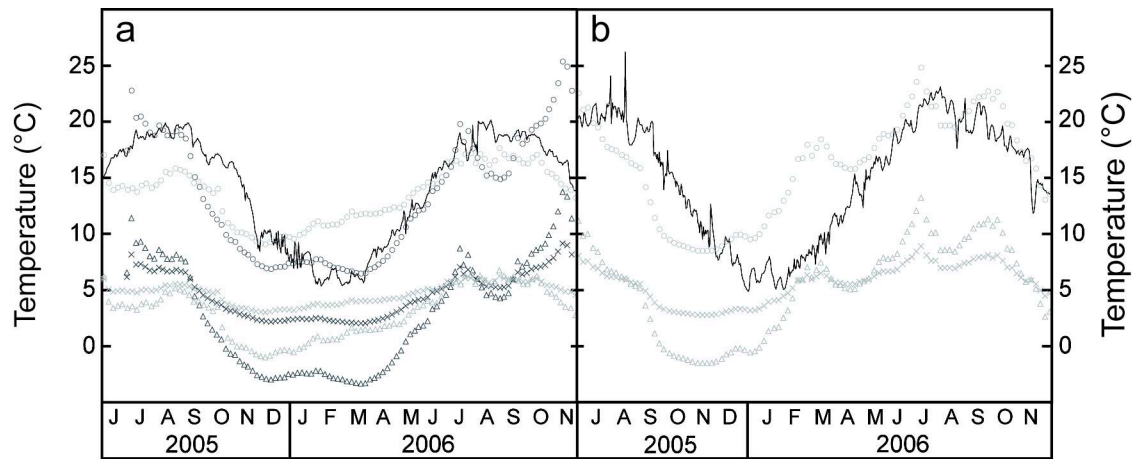
617 using this study equation (black dotted curves) and the equation from Klein et al. (1996; grey

618 dotted curves). a- Baie des Veys measured seawater temperatures (solid curve), calculated

619 SST using Mg/Ca of shells jn-gig-BV-2 (dashed curve) and jn-gig-BV-3 (dotted curve). b-

620 Marennes-Oléron measured seawater temperatures (solid curve), calculated SST using Mg/Ca

621 of shell jn-gig-MO-1 (dashed line).



622

623

624 **Table**

625 Table 1: Simplified schedule of the oyster breeding program.

Location	Shells	Birth	Hatchery Nursery	Oyster tables (before marking phase)	Marine ponds	Oyster tables (during marking phase)	Collection of oysters
Baie des Veys	C. gigas juv.	Summer 2004				February 2005	November 06
	O. edulis ad.	Summer 2003		February 2004		February 2006	November 06
Marennes Oléron	C. gigas juv.	Summer 2004				February 2005	November 06
	C. gigas ad.	March 2003	March 2003	February 2004	June 05	September 2005	November 06
	O. edulis ad.	Summer 2003		February 2004		February 2006	November 06

626

627 Table 2: Measured seawater Mg/Ca ratio, temperature and salinity at the two breeding

628 locations.

Location	Date	Mg/Ca (mmol/mol)	Temperature (°C)	Salinity (psu)
Baie des Veys	13/03/05	2.50	5.9	32.3
	27/04/05	2.66	10.2	33.7
	26/05/05	2.50	13.0	33.2
	22/06/05	2.67	16.6	33.7
	18/08/05	2.67	19.8	33.8
	07/12/05	2.66	9.9	33.1
	22/12/05	2.22	8.2	33.2
	03/02/06	2.66	5.6	33.6
	16/05/06	2.45	12.0	33.0
Marennes Oléron	09/08/06	2.68	19.7	33.9
	13/06/05	3.19	17.8	34.1
	21/06/05	3.28	18.7	34.1
	01/07/05	3.27	19.5	33.4
	20/09/05	3.27	18.0	35.2
	22/03/06	3.17	8.3	29.3
	22/05/06	3.31	12.9	29.6

629

630 Table 3: Seasonal growth rate measurements of the hinge area of *C. gigas* and *O. edulis*
631 marked shells.

Location	Group	Sample	Season	Growth rate
Baie des Veys	<i>O. edulis</i> (adult)	ad-edu-BV-1	summer	7.8 $\mu\text{m/day}$
		ad-edu-BV-2	summer	2.9 $\mu\text{m/day}$
		ad-edu-BV-3	summer	10.7 $\mu\text{m/day}$
	<i>C. gigas</i> (juvenile)	jn-gig-BV-1	summer	13.7 $\mu\text{m/day}$
			winter	19.9 $\mu\text{m/day}$
		jn-gig-BV-2	summer	16.8 $\mu\text{m/day}$
			winter	14.2 $\mu\text{m/day}$
			summer	13.2 $\mu\text{m/day}$
		jn-gig-BV-3	summer	27.4 $\mu\text{m/day}$
			summer	23.9 $\mu\text{m/day}$
Marennes- Oléron	<i>O. edulis</i> (adult)	ad-edu-MO-1	winter	15.9 $\mu\text{m/day}$
		ad-edu-MO-2	summer	20.0 $\mu\text{m/day}$
	<i>C. gigas</i> (juvenile)	ad-edu-MO-1	summer	2.0 $\mu\text{m/day}$
		ad-edu-MO-2	winter	3.4 $\mu\text{m/day}$
	<i>C. gigas</i> (adult)	ad-gig-MO-1	summer	9.8 $\mu\text{m/day}$
		ad-gig-MO-2	winter	5.6 $\mu\text{m/day}$
		ad-gig-MO-3	summer	12.9 $\mu\text{m/day}$
			ad-gig-MO-3	winter
			winter	2.5 $\mu\text{m/day}$
			summer	7.4 $\mu\text{m/day}$
			winter	2.8 $\mu\text{m/day}$

632

633 Table 4: Mean shell Mg/Ca ratios of *C. gigas* and *O. edulis* used in this study.

Location	Sample code	Number of analyses	Mg/Ca (mmol/mol) min/max	Mean \pm standard deviation (mmol/mol)
Baie des Veys	jn-gig-BV-1	394	1.25/9.92	4.37 \pm 2.05
	jn-gig-BV-2	394	0.87/9.26	3.16 \pm 1.64
	jn-gig-BV-3	398	1.52/7.13	3.42 \pm 0.85
	ad-edu-BV-1	67	0.89/5.08	2.59 \pm 1.08
	ad-edu-BV-2	39	0.96/8.07	3.64 \pm 1.65
	ad-edu-BV-3	59	0.84/5.00	2.10 \pm 0.89
Marennes-Oléron	jn-gig-MO-1	190	1.27/10.51	4.14 \pm 1.54
	ad-gig-MO-2	54	1.25/15.43	4.82 \pm 2.06
	ad-gig-MO-3	96	3.89/16.60	7.10 \pm 1.68
	ad-edu-MO-1	18	3.25/8.88	5.13 \pm 1.87
	ad-edu-MO-2	23	3.71/17.57	6.84 \pm 3.02

634

635 Table 5: Main periodicities deduced from FFT analysis of the time calibrated Mg/Ca

636 evolution curves of *C. gigas* and *O. edulis* shells (days are solar days).

	25.6-31.3	13.7-15.4
ad-edu-BV-1	-	X
ad-edu-BV-2	-	-
ad-edu-BV-3	-	-
jn-gig-BV-1	X	X
jn-gig-BV-2	X	X
jn-gig-BV-3	X	X
ad-gig-MO-1	-	-
ad-gig-MO-2	-	-
ad-edu-MO-1	-	-
ad-edu-MO-2	-	X
jn-gig-MO-1	X	X

637

638

639